

# Use of Non-Axisymmetric Specimens in Upsetting for Determining the Workability Diagram

Dragisa Vilotić<sup>1,a</sup>, Sergei Alexandrov<sup>2,b</sup>, Miroslav Plancak<sup>1,c</sup>, Aljosa Ivanisević<sup>1,d</sup>

<sup>1</sup> University of Novi Sad, Faculty of Technical Sciences, Department for Production Engineering, Trg Dositeja Obradovića 6, 21000 Novi Sad, Serbia

<sup>2</sup> A.Ishlinskii Institute for Problems in Mechanics RAS, 101-1 Prospect Vernadskogo, 119526 Moscow, Russia

<sup>a</sup> vilotic@uns.ac.rs, <sup>b</sup> sergei\_alexandrov@yahoo.com, <sup>c</sup> plancak@uns.ac.rs, <sup>d</sup> aljosa@uns.ac.rs

**Keywords:** Upsetting, Workability diagram, Ductile fracture, Metal forming.

**Abstract.** Ductile fracture criteria are often used to predict fracture initiation in metal forming processes. One of such criteria is based on the workability diagram and an average value of the triaxiality factor over the strain path. An advantage of this ductile fracture criterion is that stress invariants involved in the original criterion can be excluded when fracture occurs at a traction free surface. Thus this reduced criterion is formulated in terms of the in-surface strains. The latter can be found experimentally by means of well documented techniques. Using this property of the ductile fracture criterion under consideration it is possible to obtain points of the workability diagram by means of a series of upsetting tests. Previous studies in this field have mainly focused on axisymmetric specimens. In the present paper, upsetting of non-axisymmetric specimens by flat dies is adopted to study material workability of the steel C45E. Experimental results obtained are combined with the workability diagram determined using basic tests (Rastegaev test, upsetting of cylinder by flat dies, torsion and collar test). The motivation of using non-axisymmetric specimens is to find new strain paths which can be useful for the determination of the workability diagram.

## Introduction

Workability is the capability of material to be shaped by plastic deformation without any damage such as, for example, crack appearance. It is convenient to distinguish two groups of workability criteria, theoretical and empirical. Empirical criteria are based on experimental investigation of real forming processes and they can be represented by two variants of the workability diagram. The first variant of the workability diagram is strain based and it is a relation between the principal strains at free surface at the instant of crack appearance. This type of the workability diagram has been applied in [1-4]. The second variant of the workability diagram is stress based [5-13] and it is a relation between the strain to fracture and triaxiality ratio at the site of ductile fracture initiation. This type of the workability diagram has been used in [14-16] among others. According to [5], material workability depends on material type, material microstructure, process temperature, strain rate, stress state and other factors. A conventional quantitative measure of material workability is the effective strain to fracture ( $\phi'_e$ ), i.e. the magnitude of the effective strain at the instant of fracture initiation. For a given material whose initial micro-structure is specified and under quasi-static cold forming conditions, the workability diagram is solely dependent of the state of stress. This assumption is accepted in the present paper. In order to predict the fracture initiation in real processes, the workability diagram should be supplemented with a fracture criterion.

## Ductile fracture criterion based on the workability diagram

The workability diagram can be expressed mathematically as in [5]

$$\varphi_e^I = F(\beta) \quad (1)$$

where  $\beta$  is triaxiality ratio at the site of fracture initiation. The triaxiality ratio is defined as:

$$\beta = \frac{\sigma_x + \sigma_y + \sigma_z}{\sigma_e} = \frac{\sigma_1 + \sigma_2 + \sigma_3}{\sigma_e} \quad (2)$$

where  $\sigma_x, \sigma_y, \sigma_z$  are the normal stresses in three orthogonal directions ( $x, y, z$ );  $\sigma_1, \sigma_2, \sigma_3$  are the principal normal stresses and  $\sigma_e$  is the effective (Mises) stress. The function  $F(\beta)$  involved in Eq. 1 usually satisfies the condition  $dF/d\beta < 0$  for all  $\beta$ . By assumption, Eq. 1 is valid if  $\beta$  does not vary at the site of fracture initiation throughout the process of deformation. The function  $F(\beta)$  is usually approximated using experimental results from uniaxial tensile test,  $\beta = +1$ , torsion test,  $\beta = 0$ , and uniaxial compression test,  $\beta = -1$  [5].

In the case of non-monotonic processes the triaxiality ratio varies during the process of deformation and its average value can be used in the workability diagram to formulate a ductile fracture criterion [6, 7, 13]. This average value of the triaxiality ratio is defined by

$$\beta_{av} = \frac{1}{\varphi_e^I} \int_0^{\varphi_e^I} \beta(\varphi_e) d\varphi_e \quad (3)$$

where  $\beta(\varphi_e)$  is the dependence of the triaxiality ratio on the effective strain at the site of fracture initiation. There are two methodologies based on the flow theory of plasticity to determine the average value of the triaxiality ratio when the initiation of ductile fracture occurs at a free surface of specimens. A local Cartesian coordinates ( $x, y, z$ ) at a generic point of the traction free surface can be chosen such that its  $y$ -axis is orthogonal to the surface (Fig. 1). In this coordinate system  $\sigma_y = 0$ . Therefore, it follows from Eq. (2) that

$$\beta = \frac{\sigma_x + \sigma_z}{\sigma_e} = - \frac{1 + \frac{1+2\alpha}{2+\alpha}}{\sqrt{1 - \frac{1+2\alpha}{2+\alpha} + \left(\frac{1+2\alpha}{2+\alpha}\right)^2}} \quad (4)$$

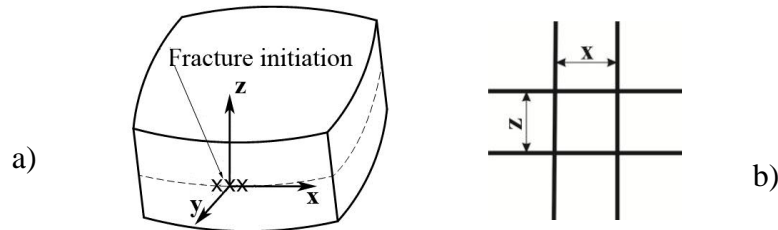


Fig. 1. Deformation of prismatic specimen (a), grid lines (b)

In this equation the coefficient  $\alpha$  is determined by

$$\alpha = \frac{d\varphi_x}{d\varphi_z}. \quad (5)$$

In order to find this coefficient, the strain path should be first found experimentally and then approximated by:

$$\varphi_x = f(\varphi_z) = A\varphi_z + B\varphi_z^2 \quad (6)$$

where  $A$  and  $B$  can be found, for example, by the least square method.

It has been shown in [17] that the average value of the triaxiality ratio is expressed through the in-surface principal strains  $\varphi_1'$  and  $\varphi_2'$  as

$$\beta_{av} = \frac{2}{\varphi_e}(\varphi_1' + \varphi_2'). \quad (7)$$

Workability analysis based on the triaxiality ratio has been carried out in a number of works. In [6], workability in upsetting of cylinders made of the steel C45 by flat and recessed dies has been analysed. Paper [7] provides some information on material workability of the steel C45E in upsetting of cylindrical and prismatic specimens by V-shape dies. In [9], workability in upsetting of prismatic specimens made of the steel C35 by cylindrical dies has been analysed. In paper [10], workability in upsetting of cylinders made of the same steel by spherical dies has been investigated. Workability in upsetting of cylinders by flat and cone-concave dies has been studied in [11]. In paper [13] results obtained by upsetting prismatic specimens of steel C45E by cylindrical and flat dies have been presented.

The present paper describes an experimental study on workability of the steel C45E. First, standard tests (cylinder upsetting, Rastegaev upsetting test, torsion and collar cylinder tests) are completed. Then, these results are supplemented with data acquired in upsetting of non-axisymmetric specimens (Fig. 2) by flat plates.

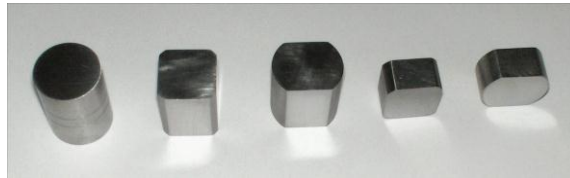


Fig. 2. Initial shape of samples (five types)





The main objective of the research is to understand advantages and perspectives of using of non-axisymmetric specimens for determining the workability limit diagram by means of upsetting with flat dies.

### **Experimental determination of workability diagram by standard tests**

The workability diagram for the steel C45E was obtained by following tests: (i) cylinder upsetting, (ii) torsion test (data from [7] were used), (iii) collar test (data from [12] were used), and (iv) Rastegaev upsetting test [13]. The methodology for determining the workability parameters is presented in [7]. Table 1 provides the triaxiality ratio and strain to fracture for different strain paths

investigated at the Laboratory for technology of plasticity, University of Novi Sad, and documented in the aforementioned papers.

Table 1. Standard tests results for the steel C45E

Test	Photos of specimens	$\beta_{av}$	$\phi_e^I$
Collar cylinder (CC) [12]		+1.21	0.32
Torsion (T) [7]		0.00	0.73
Cylinder Upsetting (BC) [7]		-0.40	1.12
Rastegaev Test (RT) [13]		-0.94	1.74

The description of the Rastegaev method is presented in [13]. The initial diameter of the specimen was 20mm and the initial height was 26mm. Shallow cylindrical grooves (0.3 mm depth) were made at the top and bottom of the contact surfaces of specimens and were filled with stearin before testing to reduce friction.

### Material workability in upsetting of non-axisymmetric specimens by flat dies

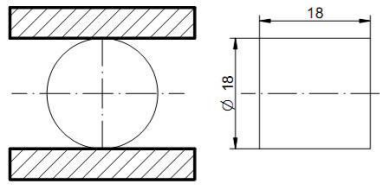

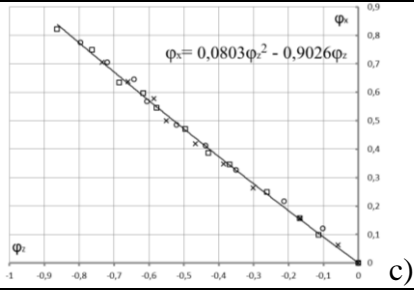
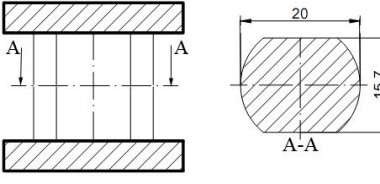

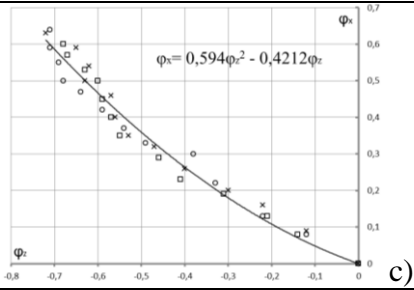
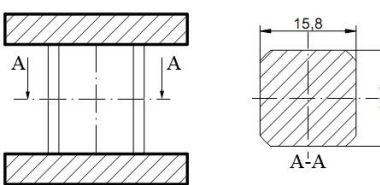

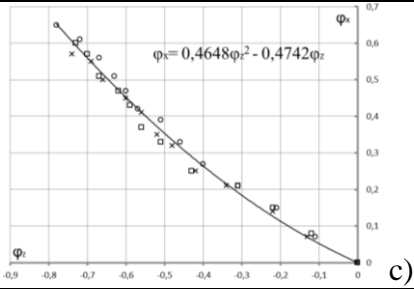
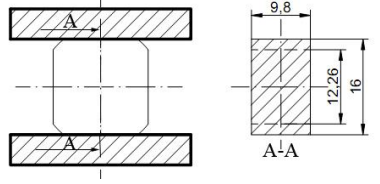

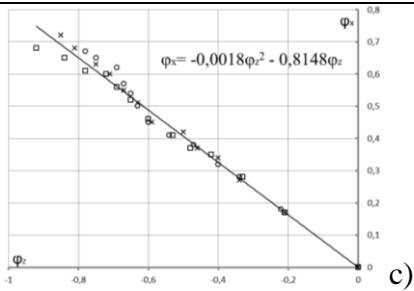
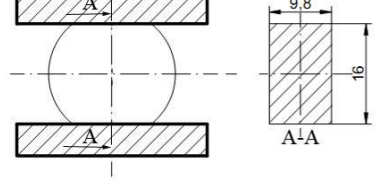

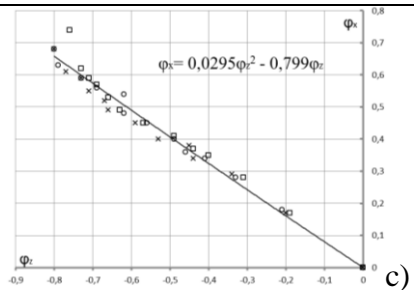
The objective of this experimental program was to verify material workability under different stress state conditions, which resulted from specific geometries of non-axisymmetric specimens subjected to upsetting by flat dies.

The site of fracture initiation in all cases was at the intersection of two planes of symmetry on the traction free surface. In order to use Eq. 7, it is necessary to determine the in-surface principal strains. To this end two pairs of grid lines were applied in the vicinity of the intersection of two planes of symmetry. These lines formed a square (Fig. 1b) with its side of 3 mm before deformation. Measuring the distance between the lines at several stages of the process the in-surface principal strains at each stage were found. Having these strains and the instant of fracture initiation determined experimentally five points of the workability diagram were found.

Upsetting of specimens (Type 1 – Type 5) was performed incrementally on hydraulic press (0.1 mm/s tool velocity) by flat tools. Specimens were lubricated with mineral oil prior to compression. End of the deformation process is defined with appearing of cracks on the outer surface of the specimen.

After each compression phase, the size of the grid defined by its width ( $x$ ) and height ( $z$ ) (Fig. 1b) was precisely measured. The strain components were calculated as  $\phi_x = \ln(x/x_0)$  and  $\phi_z = \ln(z/z_0)$  based upon these measurements. Three experiments for each case were conducted. In Table 2 relevant experimental results for five types of specimens used are presented.

Table 2. Experimental data for upsetting of non-axisymmetric specimens by flat dies: a) scheme of process, b) photos of specimen before and after deformation, c) strain path diagram

<p>a)</p> 	<p>b)</p> 	<p>c)</p>  $\varphi_x = 0,0803\varphi_z^2 - 0,9026\varphi_z$
Type 1		
<p>a)</p> 	<p>b)</p> 	<p>c)</p>  $\varphi_x = 0,594\varphi_z^2 - 0,4212\varphi_z$
Type 2		
<p>a)</p> 	<p>b)</p> 	<p>c)</p>  $\varphi_x = 0,4648\varphi_z^2 - 0,4742\varphi_z$
Type 3		
<p>a)</p> 	<p>b)</p> 	<p>c)</p>  $\varphi_x = -0,0018\varphi_z^2 - 0,8148\varphi_z$
Type 4		
<p>a)</p> 	<p>b)</p> 	<p>c)</p>  $\varphi_x = 0,0295\varphi_z^2 - 0,799\varphi_z$
Type 5		

Strain path curves for specimens Type 1 – Type 5 provided in Fig. 3 were drawn based upon data from Table 2, together with strain paths from the standard tests (Table 1).

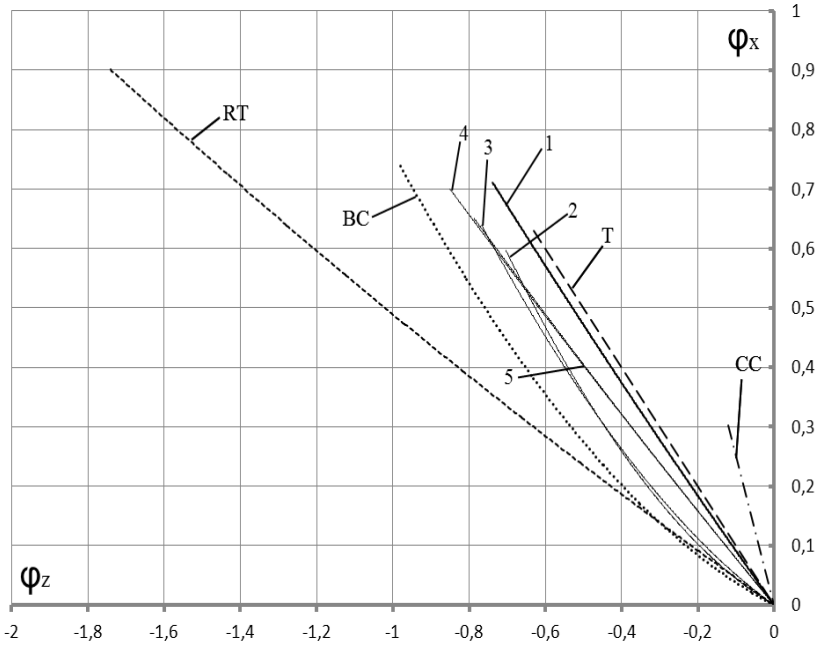


Fig. 3. Strain path for different tests: RT – Rastegaev test, BC – cylinder upsetting, T – torsion test, CC – collar cylinder test, 1– Type 1, 2 –Type 2, 3 –Type 3, 4 –Type 4, 5 – Type 5

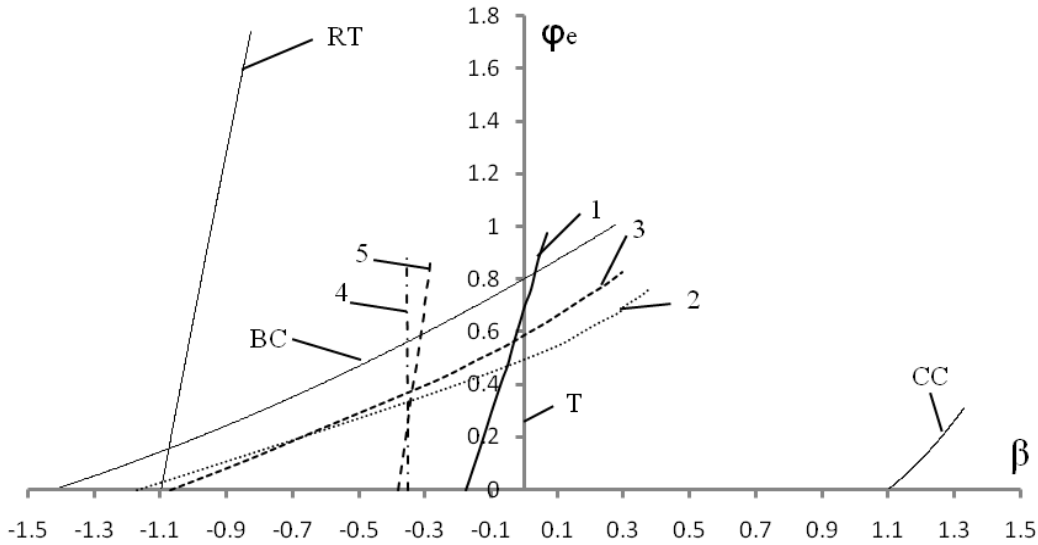


Fig. 4. History of triaxiality ratio for different specimens: RT – Rastegaev test, BC – cylinder upsetting, T – torsion test, CC – collar cylinder test, 1– Type 1, 2 –Type 2, 3 –Type 3, 4 –Type 4, 5 – Type 5

Strain path data for particular specimen's series were used as input parameters for calculation of values of the triaxiality ratio at different upsetting stages by Eq. 4. The history of the triaxiality ratio for different specimens is presented in Fig. 4. The average value of the triaxiality ratio was calculated by means of Eq. 3 and these data along with appropriate values of strains to fracture are inserted in the forming limit diagram for the steel C45E (Fig. 5).

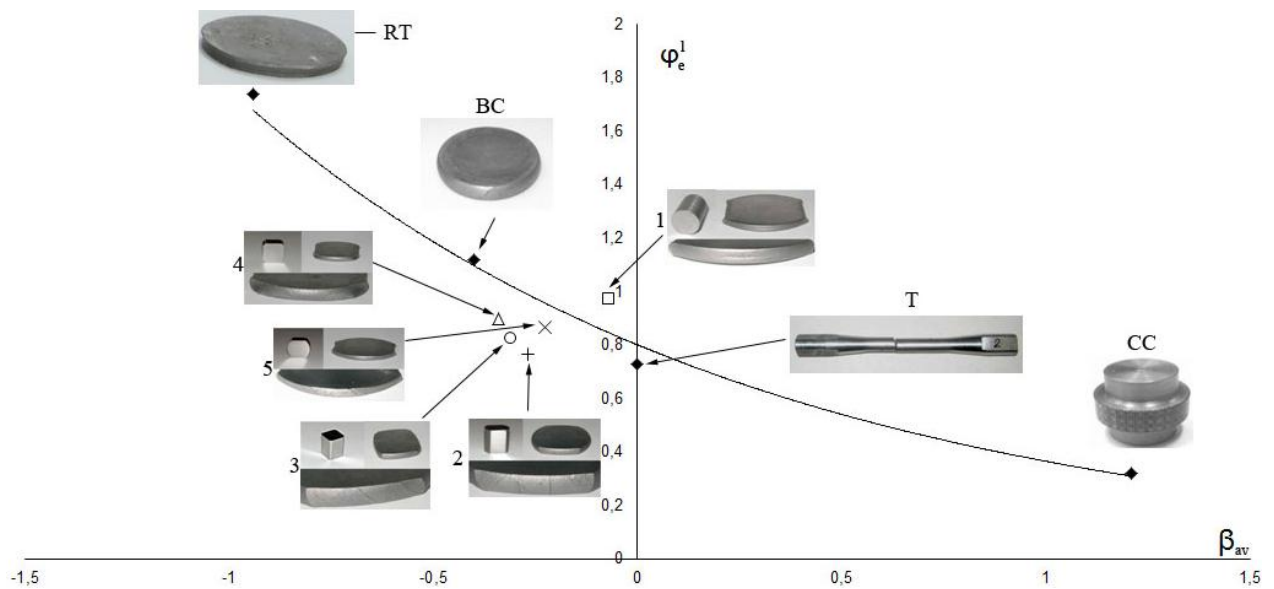


Fig. 5. Forming limit diagram of steel C45E: RT–Rastegaev test, BC–cylinder upsetting, T–torsion test, CC–collar cylinder test, 1–Type 1, 2–Type 2, 3–Type 3, 4–Type 4, 5–Type 5

### Discussion and conclusions

Material flow in upsetting of non-axisymmetric specimens by flat dies differs from that in axial upsetting of cylinders by flat dies and in the Rastegaev upsetting test. Therefore, the strain path (Fig. 3) and the history of the triaxiality ratio (Fig. 4) in these processes differ as well.

The strain paths (Fig. 3) and the history of the triaxiality ratio (Fig. 4) show that non-axisymmetric specimens (Type 1 – Type 5) can be classified into three sub-groups: a) specimen of Type 1, b) specimens of Type 2 and 3 and c) specimens of Type 4 and Type 5.

The specific strain path of specimens of Type 1 (Fig. 3, curve 1) has a consequence that this upsetting model is similar to the torsion test (Fig. 5).

Specimens of Type 2 and Type 3 belong to the category of upsetting processes with a distinctive change of stress-strain state which is presented, for example, in the axial compression of cylinders with friction at the contact surfaces.

The strain path and the history of the triaxiality ratio for specimens of Type 4 and 5 resemble to the diagrams of specimen 1 (Fig. 3 and Fig. 4), but, there is a significant difference regarding final values of strain components and the triaxiality ratio.

Based upon the data regarding material workability in compression of non-axisymmetric specimens by flat dies (Fig. 5) it is evident that all these models are located between standard upsetting of cylinders and torsion. Stress-strain state and limit workability results of these models differ from the results obtained in the process of cylinder upsetting by the Rastegaev method and axial upsetting of cylinders including friction. For the experimental determination of workability diagram specimens of Type 1, Type 4 and Type 5 are recommended. Specimens of Type 2 and Type 3 produce the data similar to that that can be obtained by axial upsetting of cylinders by flat dies.

### References

- [1] P. Gänser: Free-surface ductility in bulk forming processes, *International Journal of Plasticity*, 17 (2001), 755-772.
- [2] A. R. Ragab: Fracture limit curve in upset forging of cylinders, *Materials Science and Engineering*, A334 (2002), 114-119.

- [3] J. Landre, A. Pertence, P. R. Cetlin, J. M. C. Rodrigues, P. A. F. Martins: On the utilization of ductile fracture criteria in cold forging, *Finite Elements in Analysis and Design*, 39 (2003), 175-186.
- [4] G. Dieter, H. Kuhn, L. Semiatin: Chapter 2 Bulk Workability of Metals, Chapter 3 Evolution of Microstructure during Hot Working, *Handbook of Workability and Process Design*, ASM International, Material Park Ohio (2003), 22-39 .
- [5] V. Vujovic, A. Shabaik: Workability Criteria for Ductile Fracture, *Trans. ASME J. Engng. Mater. Technol.*, 108 (1986), 245-249.
- [6] D. Vilotic, M. Plancak, Đ. Cupković, S. Alexandrov, N. Alexandrov: Free Surface Fracture in Three Upsetting Tests, *Experimental Mechanics*, 46 (2006), 115-120.
- [7] D. Vilotić, S. Alexandrov, M. Plančak, D. Movrin, A. Ivanišević, M. Vilotić: Material Workability at Up-setting by V-Shape Dies, *Steel Research International, Special Edition*, (2011), 923-928.
- [8] S. Alexandrov, D. Vilotic: Theoretical and Experimental Analysis of Fracture Initiation at the Free Surface in Upsetting by Conical Dies, *Steel Research International*, 2 (2008), 375-381.
- [9] S. Alexandrov, N. Chikanova, D. Vilotic: Compression of a Block Between Cylindrical Dies and its Application to the Workability Diagram, *Studies in Applied Mechanics, Advanced Methods in Materials Processing Defects*, 45 (1997), 247-256.
- [10] D. Vilotic, N. Chikanova, S. Alexandrov: Disk Upsetting Between Spherical Dies and its Application to the Determination of Forming Limit Curves, *Journal Strain Analysis*, 34 (1999), 17-22.
- [11] D. Vilotic, M. Plancak, S. Grbic, S. Alexandrov, N. Chikanova: An approach to determining the workability diagram based on upsetting tests, *Fatigue Fract. Engng. Mater. Struct.*, 26 (2001), 305-310.
- [12] S. Alexandrov, D. Vilotic, Z. Konjovic, M. Vilotic: An Improved Method for Determining the Workability Diagram, submitted to *Experimental Mechanics*, (2011).
- [13] D. Vilotic, S. Alexandrov, M. Plancak, M. Vilotic, A. Ivanisevic, I. Kacmarcik: Material Formability at Upsetting by Cylindrical and Flat Dies, *Steel Research International*, in press.
- [14] V. L. Kolmogorov: *Mehanika obrabotki metallov davleniem*, UPI, Ekaterinburg, (2001), 664-718.
- [15] M. Brandes in: *The Mechanical behaviour of Materials under Pressure*, edit by H. LI. Pugh The Applied science Publisher, London (1970), 236-298.
- [16] D. Breuer: Bestimmung des Formänderungsvermögens bei der Kaltmassivumformung, *Berichte aus der Produktionstechnik*, band 19/2007, Sharker Verlag, (2007), 11-13.
- [17] S. Alexandrov, D. Vilotic, R. Goldstein, N. Chikanova: The Determination of the Workability Diagram, *Mechanics of Solids*, 34 (1999), 118-125.

**Acknowledgements:** This paper is a part of the investigation within the project EUREKA E!5005 financed by Serbian Ministry of Education and Science and RFBR-12-08-01104 (Russia).